QUANTUM VACUUM FLUCTUATIONS IN INORGANIC COMPOUND CdSe

FLUCTUACIONES DE VACÍO CUÁNTICO EN EL COMPUESTO INORGÁNICO CdSe

Luciano Nascimento*, Carlos H. G. Béssa, Eduardo M. R. dos Passos

Federal University of Campina Grande – Academic Unit of Physical, Postgraduate Program in Physical, Av. Aprígio Veloso, 882 – Bloco CY 2 – Bodocongó CEP: 58.429-900 / Campina Grande – Paraíba, Brazil.

(Recibido: 07/2022. Aceptado: 10/2022)

Abstract

In the present work, we study the quantum vacuum fluctuations at finite temperature in the propagation of light in nonlinear optical media. We present nonlinear materials, that have the second-order electrical susceptibility tensor, and the fluctuating effective refractive index caused by fluctuating vacuum electric fields. Likewise, we study the fluctuations of the vacuum, which led to the contributions of thermal and mixed fluctuations being associated with a faithful test function to perform the calculations, in contrast to the Lorentzian distribution. We show the contribution of thermal and mixed fluctuations to time-of-flight fluctuations compared to the contributions of vacuum fluctuations. The result reveals a numerical estimate performed on cadmium selenide (CdSe) suggesting that the effects of fluctuations can cause uncertainty in time of flight due to quantum vacuum fluctuations in terms of thermal and mixed fluctuations.

Keywords: quantum vacuum fluctuations, electric field, light propagation.

*luciano.fisicacex@gmail.com doi: https://doi.org./10.15446/mo.n66.103486

Resumen

En el presente trabajo se estudiaron las fluctuaciones del vacío cuántico a temperatura finita en la propagación de la luz en medios ópticos no lineales. Se presentan materiales no lineales que tienen el tensor de susceptibilidad eléctrica de segundo orden y el índice de refracción efectivo fluctuante causado por campos eléctricos de vacío fluctuantes. De igual manera, se estudiaron las fluctuaciones del vacío, lo que llevó a asociar las contribuciones de las fluctuaciones térmicas y mixtas a una función de prueba fiel para realizar los cálculos, en contraste con la distribución lorentziana. Se muestra la contribución de las fluctuaciones térmicas y mixtas a las fluctuaciones del tiempo de vuelo en comparación con las contribuciones de las fluctuaciones del vacío. El resultado arrojó una estimación numérica realizada en seleniuro de cadmio (CdSe) que sugiere que los efectos de las fluctuaciones pueden causar incertidumbre en el tiempo de vuelo debido a las fluctuaciones del vacío cuántico en términos de fluctuaciones térmicas y mixtas.

Palabras clave: fluctuaciones del vacío cuántico, campo eléctrico, propagación de la luz.

Introduction

The existence of quantum fluctuations is of utmost importance, particularly in the context of quantum electrodynamics that, even in the absence of electric charges and currents, there exists a fluctuating electromagnetic field that has a certain non-zero energy level [1]. A fluctuating electric field in a nonlinear material causes fluctuations in the background field, changing the phase velocity of the probe field coupled to the background field through the nonlinearity of the material medium, being an analogous model for evolving quantum gravitation effects quantum optics [2].

Vacuum fluctuations of the electromagnetic field are responsible for several observed phenomena, such as the Casimir effect (and the dynamic Casimir effect), the Lamb shift and spontaneous emission, to name a few. Vacuum fluctuations are associated with

the quantum field operators of the electric field, which are only significant if the operators have been averaged over time with a smooth sampling function [3–5]. In general, these distributions tend to fall more slowly than a Gaussian function, which increases the likelihood of large fluctuations, and depend significantly on the choice of the sampling function. Also, the sampling function for vacuum fluctuations in a dielectric may depend on the geometry of the material. However, there are strong debates about vacuum fluctuations as temporary events, because vacuum fluctuations are as real as thermal fluctuations, but are often not noticed due to strong anticorrelations.

Therefore, with respect to the vacuum, it does not necessarily correspond to a space without matter, but to the lowest energy state of the quantized electromagnetic field, so that a natural question is that thermal fluctuations are unavoidable in a real experiment, even in the vacuum and with the participation of the contributions of thermal and mixed fluctuations to the time of flight. Lorentz-Heaviside units can be considered normalizers with $\hbar = c = k_B = 1$ and $\epsilon_o = \mu_o = 1$ [6]. The Heisenberg uncertainty principle imposes a condition that the ground state energy of the field is non-zero, which implies a fluctuating electromagnetic field. The purpose of this article is to obtain the effects of finite temperature at very low ambient temperature, observing the effects of vacuum fluctuations in second-order non-linear media in an inorganic compound material, cadmium selenide (CdSe).

Flight Time in a Nonlinear Optical Material

Classical propagation speed

A nonlinear dielectric material is one in which the electric polarization vector is a nonlinear function of the electric field and can be written as [7],

$$P_i = \epsilon_o \left(\chi_{ij}^{(1)} E_j + \chi_{ijk}^{(2)} E_j E_k + \chi_{ijk}^{(3)} E_j E_k E_l + \cdots \right), \qquad (1)$$

where we define the electrical susceptibilities tensors $\chi_{ij}^{(1)}$, $\chi_{ijk}^{(2)}$ and $\chi_{ijkl}^{(3)}$ first, second and third order, respectively. Generally speaking,

$\chi^{(1)}$ is dimensionless, $\chi^{(3)} = \left(\frac{m^2}{V^2}\right) \ll \chi^{(2)} = \left(\frac{m}{V}\right) \ll 1$ and therefore this approximation is optimal for non-intense fields. The second and higher order susceptibilities lead to a nonlinear wave equation for the electric field can be expressed as, using eq.(1) we have that [8],

$$\nabla^2 E_i - \frac{\partial^2 E_i}{\partial t^2} = \frac{\partial^2}{\partial t} \left(\chi_{ij}^{(1)} E_j + \chi_{ijj}^{(2)} E_j E_k \right), \tag{2}$$

Consider a pulse of light that passes through a nonlinear optical medium as shown in Figure 1.

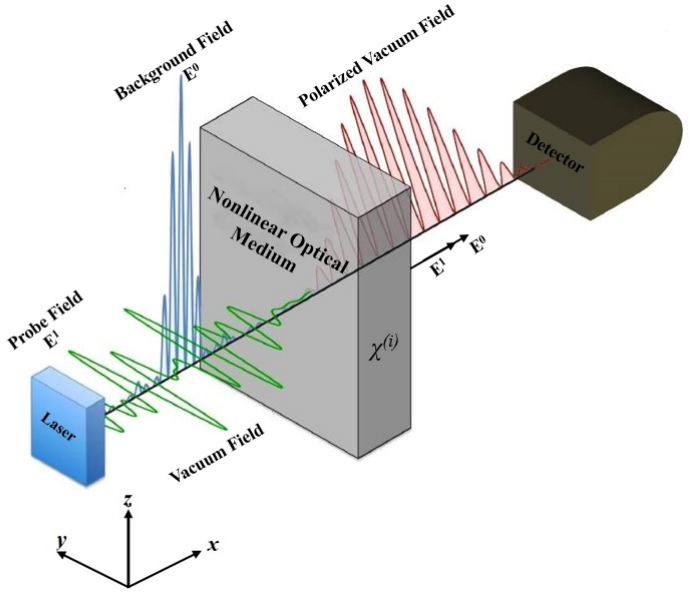

FIGURE 1. A pulse of light passing through a non-linear optical medium.

We assume that the total electric field can be written as the sum of a background field $\mathbf{E}^0$ and a smaller, but more rapidly varying probe field $\mathbf{E}^1$ in

$$\mathbf{E} = \mathbf{E}^0 + \mathbf{E}^1, \tag{3}$$

where $|E_0| \ll |E_1|$ but $\left|\dot{E}^1/E^1\right| \gg \left|\dot{E}^0/E^0\right|$. Both $\mathbf{E}^0$ and $\mathbf{E}^1$ satisfy nonlinear equations with a coupling term between them. Here the background field describes the vacuum mode of the quantized electric field, which is approximated as a linear field in

nearly isotropic materials, so we see $\chi_{ij}^{(1)} \approx \delta\chi^{(1)}$. However, if the second-order susceptibility is small enough, we can consider the equation for $\mathbf{E}^0$ approximately linear. These coupled averages of the nonlinearity of an applied external electric field of the type $E_i^0(\mathbf{x}, t)$ is called the background field. The electric field associated with the light pulse is denoted by the vector $\mathbf{E}^1$, which we choose to be polarized in the z direction and propagating in the x direction, that is, $\mathbf{E}^1 = \mathbf{E}^1(x, t)\,\hat{\mathbf{z}}$. Furthermore, we assume that the proving field is smaller in magnitude than the background field, but varies much more rapidly. In this case, $\mathbf{E}^1$ obeys a linearized wave equation [9],

$$\frac{\partial^2 E^1}{\partial x^2} - \frac{1}{v_f^2}\frac{\partial^2 E^1}{\partial t^2} = 0, \tag{4}$$

Here v_f^2 is the phase velocity of the wave, which is given by

$$v_f^2 = \frac{1}{n_p^2}\left(1 + 2\gamma_i E_i^0 + \gamma_{ij} E_i^0 E_j^0\right)^{-1}, \tag{5}$$

$$n_p = \left(1 + \chi_{zz}^{(1)}\right)^{\frac{1}{2}}, \tag{6}$$

where in eq.(6), n_p is the refractive index of the medium measured by the probe pulse when only linear effects occur, and we define the following coefficients [10],

$$\gamma_i = \frac{1}{n_p^2}\left(\frac{\chi_{zzi}^{(2)} + \chi_{ziz}^{(2)}}{2}\right), \tag{7}$$

$$\gamma_{ij} = \frac{1}{n_p^2}\left(\frac{\chi_{zzij}^{(3)} + \chi_{zizj}^{(3)} + \chi_{zijz}^{(3)}}{3}\right). \tag{8}$$

Eq.(5) shows that the background field couples to the nonlinearities of the medium, affecting the speed of the waves that propagate through it. Note, that scattering can be neglected, so that the group velocity of a wave packet is approximately equal to the phase velocity. Therefore, the flight time of a probe pulse traveling a distance d in the direction x will be given by [11],

$$t_d = n_p \int_0^d \left(1 + \gamma_i E_i^0(\mathbf{x},t) + \mu_{ij} E_i^0(\mathbf{x},t)\, E_j^0(\mathbf{x},t)\right) dx, \qquad (9)$$

with

$$\mu_{ij} = \frac{1}{2}\left(3\gamma_{(ij)} - \gamma_i\gamma_j\right). \qquad (10)$$

Note, that the term between the parentheses in eq.(8) involves two indices that denotes symmetrization, that is,

$$2\gamma_{(ij)} = \gamma_{ij} + \gamma_{ji}. \qquad (11)$$

When writing eq.(11), we assume that the nonlinear effects are small, so we can expand into a Taylor series of type $1/v_f$ of eq.(5) for the first-order terms in eq. (5) in $\gamma_{(ij)}$ and second-order terms in γ_j. Furthermore, we only consider the integrand in eq.(9) when evaluated at $t = n_p x$, which is a pulse of light traveling at the speed $1/n_p$, being determined by the linear susceptibility of the material medium.

Vacuum Fluctuations and Switching

As we saw earlier, the equation eq.(9) is an expression that describes the time of flight and studies the effects of fluctuations in the electric field of vacuum as the background field. In this case, $\mathbf{E}^0$ becomes the electric field operator quantized and t_d defined in eq.(3) becomes an operator, where the quadratic term in $\mathbf{E}^0$ is generally considered to be ordered normal of the type: $E_i^0(\mathbf{x},t)\, E_j^0(\mathbf{x},t) \rightarrow : E_i^0(\mathbf{x},t)\, E_j^0(\mathbf{x},t) :$. This leads to a finite mean flight time, which in the vacuum state is, for the main order [12],

$$\langle t_d \rangle = n_p d, \qquad (12)$$

and and our primary interest will be in the variance of the flight time,

$$(\triangle t_d)^2 = \left\langle {t_d}^2 \right\rangle - \langle t_d \rangle^2. \qquad (13)$$

Note that this quantity is independent of the selection of vacuum conditions under which normal ordering is made. However, if we perform a certain change in state, and add a certain number C, to the operator t_d, such that $t_d \rightarrow t_d + C$, it is easily verified that the

right side of eq. (13) has not been changed. A change in vacuum state may slightly change the average delay time,$\langle t_d \rangle$, but does not change the variation in flight time. However, this amount is only finite if the field operators were averaged with a test function. In the present context, the density profile of the dielectric plate naturally defines a suitable function. Let $F(x)$ be a profile function that satisfies eq. (14) and is normalized,

$$\frac{1}{d}\int_{-\infty}^{+\infty} F\left(x\right) dx = 1. \tag{14}$$

Now the delay time operator can be written as

$$t_d = n_p \int_{-\infty}^{+\infty} \left[1 + \gamma_i E_i^0\left(x,\right) + \mu_{ij} : E_i^0\left(\mathbf{x},t\right) E_j^0\left(\mathbf{x},t\right) :\right] F(x) dx. \tag{15}$$

Hence, the variation in flight time becomes [13]

$$\begin{aligned}(\Delta t_t)^2 = {n_p}^2 &\int_{-\infty}^{+\infty} dx F(x) \\ &\times \int_{-\infty}^{+\infty} dx' F(x') [\gamma_i \gamma_j \left\langle E_i^0(\mathbf{x},t) E_j^0(\mathbf{x}',t')\right\rangle + \\ &+ \mu_{ij}\mu_l \left\langle : E_i^0(\mathbf{x},t) E_j^0(\mathbf{x},t) :: E_l^0(\mathbf{x}',t') E_m^0(\mathbf{x}',t')\right] .\end{aligned}$$

The definition of normal order is

$$: E_i^0(\mathbf{x},t) E_i^0(\mathbf{x}',t') := E_i^0(\mathbf{x},t) E_i^0(\mathbf{x}',t') - \left\langle E_i^0(\mathbf{x},t) E_i^0(\mathbf{x}',t')\right\rangle , \tag{16}$$

and using Wick's Theorem [13], we are left with

$$\begin{aligned}\left\langle : E_i^0(\mathbf{x},t) E_j^0(\mathbf{x},t) :: E_l^0(\mathbf{x}',t') E_m^0(\mathbf{x}',t') : \right\rangle = &\left\langle E_i^0(\mathbf{x},t) E_l^0(x',t'\right\rangle \times \\ &\times \left\langle E_j^0(\mathbf{x},t) E_m^0(\mathbf{x}',t'\right\rangle + \\ &+ \left\langle E_i^0(\mathbf{x},t) E_m^0(\mathbf{x}',t')\right\rangle \times \\ &\times \left\langle E_j^0(\mathbf{x},t) E_l^0(\mathbf{x}',t')\right\rangle\end{aligned} \tag{17}$$

Thus, the time of flight variance can be expressed as an integral involving the electric field correlation functions. This double integral is above the spacetime volume of the probe pulse wave packet. The background field is set up in a given quantum state, and therefore fluctuates. We will assume that the wave packet is sufficiently localized around this world line to be able to neglect integrations over the spatial directions transverse to the x-direction. In this limit, we are averaging the electric field and the square of the electric field along the universe line of an observer moving with the probe pulse. In the remaining frame of this observer, field operators are just averaging over time. Once we take the transverse coincidence limit of the spatial directions, as the electric field correlation functions for a non-dispersive isotropic material become [14],

$$\left\langle E_x^0(x,t)E_x^0(x',t')\right\rangle = \frac{1}{\pi^2 {n_b}^3\left[(\Delta x)^2 - \frac{(\Delta t)^2}{{n_b}^2}\right]^2}, \tag{18}$$

$$\left\langle E_y^0(x,t)E_y^0(x',t')\right\rangle = \left\langle E_z^0(x,t)E_z^0(x',t')\right\rangle = \frac{(\Delta x)^2 + \frac{(\Delta t)^2}{{n_b}^2}}{\pi^2 {n_b}^3\left[\frac{(\Delta t)^2}{{n_b}^2} - (\Delta x)^2\right]^3}, \tag{19}$$

and

$$\left\langle E_i^0(x,t)E_j^0(x',t')\right\rangle = \begin{cases} 1 & \text{, if } i=j \\ 0 & \text{, if } i\neq j \end{cases}, \tag{20}$$

where $\Delta x = x - x'$ and with $\Delta t = t - t' - i\varepsilon$ with $\varepsilon > 0$ and n_b is the index of refraction measured by the background field E_i^0.

Fractional Variance in the Flight Time

Using the above results and remembering that the integrations in eq.(15) are performed along the path of the background pulse, given by $t = n_p x$, we get the following

$$(\Delta t_d)^2 = \int_{-\infty}^{+\infty} dx F(x) \int_{-\infty}^{+\infty} dx' F(x') \left[\frac{\alpha_1}{(\Delta x)^4} + \frac{\alpha_2}{(\Delta x)^8}\right], \tag{21}$$

where Δx is understood to have a small negative imaginary part. Here, we set the parameters α_1 and α_2 as [15]

$$\alpha_1 = \frac{n_b {n_p}^2}{\pi^2({n_p}^2 - {n_b}^2)^2}\left[{\gamma_x}^2 + \left({\gamma_y}^2 + {\gamma_z}^2\right)\frac{({n_p}^2 + {n_b}^2)}{({n_p}^2 - {n_b}^2)}\right], \tag{22}$$

$$\alpha_2 = \frac{2{n_b}^2{n_p}^2}{\pi^4({n_p}^2 - {n_b}^2)^4}\left[\mu_{xx}^2 + \left(\mu_{yy}^2 + \mu_{zz}^2 + 2\mu_{zy}^2\right) \times \frac{\left({n_p}^2 + {n_b}^2\right)}{\left({n_p}^2 - {n_b}^2\right)} + \right.$$
$$\left. + 2\left(\mu_{xy}^2 + \mu_{xz}^2\right)\frac{\left({n_p}^2 + {n_b}^2\right)}{\left({n_p}^2 - {n_b}^2\right)}\right]. \tag{23}$$

A Choice for the Switching Function

We want to choose a suitable smooth switching function that represents the transitions that occur when the background pulse enters and leaves the medium. Let's make use of the lorentzian distribution, to build an appropriate test function. It will be useful to have two parameters, one (d) describing the slab width and one (($b < d$)) describing the effective length along which the nonlinearity changes smoothly as the pulse enters and exits, one relative to the crystal size, and the other measuring how fast the effect is activated [15]. There are several options for this function. Here we use a function $F_{b,d}(x)$ defined by [16]

$$F_{b,d}(x) = \frac{1}{\pi}\left[arctan\left(\frac{x}{b}\right) + arctan\left(\frac{dx}{b}\right)\right]. \tag{24}$$

The derivative of this function with respect to x is the sum of two Lorentzian functions.

$$\frac{dF_{b,d}(x)}{dx} = \frac{1}{\pi}\left[\frac{b}{b^2 + x^2} - \frac{b}{b^2 + (xd)^2}\right]. \tag{25}$$

Note that $F_{b,d}(x)$ is the integral from minus infinity to x of the function defined by the difference of two lorentzians, one centered at the origin with parameter b and the other shifted a distance d from the origin, also with parameter b,

$$\int_{-\infty}^{+\infty} F_{b,d}(x)dx. \tag{26}$$

The Figure 2, illustrated below, shows some overlay graphs of the function $F_{b,d}(x)$ for some ratio values $\frac{b}{d}$. The parameter b describes the distance at which $F_{b,d}(x)$ changes from its minimum values to its maximum values and vice versa. Note that when $b \to 0$ we retrieve a step function, as expected. This suggests that we calculate the distance

between the first two points of maximum curvature of the graph. For this reason, if we keep only the first *arcotan*, we find that this distance is given by a factor of $\frac{2b}{\sqrt{3}}$.

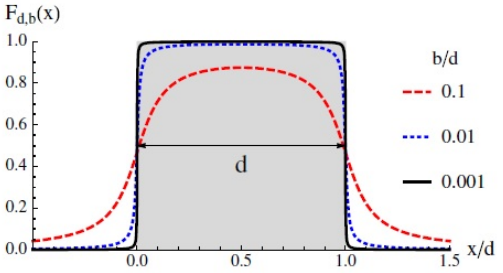

FIGURE 2. Graphs of the function $F_{b,d}(x)$.

The analysis of the parameter b measures how fast is the function $F_{b,d}(x)$ that links the effect on the regime that the material does not suffer any kind of dispersion. This result generalizes, and the contribution of third-order nonlinear susceptibility, and giving a general expression for the flight time described by the profile of the function $F(x)$. The integrals that appear in eq.(27) can be evaluated by boundary integration, with $\Delta x = x - x' - i\varepsilon$, where $\varepsilon > 0$ makes the mode sums absolutely convergent and is always associated with the refractive index measured by the background field E_i^0. The results, and their asymptotic forms when $b \ll d$, are

$$\int_{-\infty}^{+\infty}\int_{-\infty}^{+\infty} dxdx' F_{d,b}(x)F_{d,b}x'\frac{1}{\Delta x^4} = \frac{d}{12b^2}\frac{(d^2+12b^2)}{(d^2+4b^2)^2}\frac{1}{12b^2}, \tag{27}$$

$$\int_{-\infty}^{+\infty}\int_{-\infty}^{+\infty} dxdx' F_{d,b}(x)F_{d,b}x'\frac{1}{\Delta x^8} \cong \frac{1}{1344b^6}. \tag{28}$$

If we assume that $b \ll d$, and use the asymptotic forms above, we get

$$(\Delta t_d)^2 \approx \frac{\alpha_1}{12b^2} + \frac{\alpha_2}{1344b^6}. \tag{29}$$

We define the square fractional variance in the background field flight time as

$$\delta^2 = \frac{(\Delta t_d)^2}{\langle t_d\rangle^2} \approx \frac{\alpha_1}{12{n_p}^2d^2b^2} + \frac{\alpha_2}{1344{n_p}^2d^2b^6}. \tag{30}$$

So, let's create a mechanism by which the test function filters the modes of the field, associated with an operator $\hat{t}_d$ that appears as follows

$$\int_{-\infty}^{+\infty} F_{b,d}(x)\hat{E}_i(x)dx, \tag{31}$$

Let's use Parseval's identity to transform the integral from the configuration space to the reciprocal space. Therefore, the field modes are typically modulated through the Fourier transform of $F_{b,d}(x)$. In this way, the analysis of the transform carries significant information about the model validity regime. Using the transform calculation we have that,

$$\tilde{F}_{b,d}(k) = \int_{-\infty}^{+\infty} \frac{1}{\sqrt{2\pi}} F_{b,d}(x)e^{-ikx}dx. \tag{32}$$

Using the fact that,

$$f_{b,d}(x) = \frac{dF_{b,d}}{dx} = \frac{1}{\pi}\left[\frac{b}{b^2+x^2} - \frac{b}{b^2+(xd)^2}\right], \tag{33}$$

let's use integration by parts and rewrite $\tilde{F}_{b,d}$ as

$$\begin{aligned}
\tilde{F}_{b,d}(k) &= \int_{-\infty}^{+\infty} \frac{1}{\sqrt{2\pi}} F_{b,d}(x)e^{-ikx}dx \\
&= \frac{iF_{b,d}(x)e^{-ikx}}{\sqrt{2\pi}k}\Bigg|_{-\infty}^{+\infty} - \frac{i}{\sqrt{2\pi}k}\int_{-\infty}^{+\infty} f_{b,d}(x)e^{-ikx}dx \\
&= -\frac{i}{\sqrt{2\pi}k}\frac{b}{\pi}\left[\int_{-\infty}^{+\infty}\frac{e^{-ikx}}{b^2+x^2}dx - \int_{-\infty}^{+\infty}\frac{e^{-ikx}}{b^2+(xd)^2}dx\right] \\
&= -\frac{i}{\sqrt{2\pi}k}\frac{b}{\pi}\left[\int_{-\infty}^{+\infty}\frac{e^{-ikx}}{b^2+x^2}dx - e^{-ikd}\int_{-\infty}^{+\infty}\frac{e^{ikx}}{b^2+x^2}dx\right] \\
&= -\frac{i}{\sqrt{2\pi}k}\frac{b}{\pi}\left(1-e^{-ikd}\right)\int_{-\infty}^{+\infty}\frac{e^{-ikx}}{b^2+x^2}dx.
\end{aligned}$$

This integral can be calculated using the Residues Theorem. For this, it suffices to consider the cases where $k \geqslant 0$ and $k < 0$ separately. We can therefore see how the b parameter acts as a filter on the field modes through the exponential attenuation in eq.(34), obtained directly from the calculation of the Fourier Transform. Note that in the case where there is only vacuum, even if the test field is composed of more energetic modes than the background field, this condition means that the number of modes that contributes to the background field is large enough. Probe pulses are only sensitive to vacuum fluctuations that occur in a finite time interval, thus producing a non-zero effect despite the vacuum fluctuations'tendency to be anticorrelated. So the result is

$$\int_{-\infty}^{+\infty} \frac{e^{-ikx}}{b^2+x^2} dx = \frac{\pi}{b} e^{-|k|b}. \tag{34}$$

Lastly,

$$\tilde{F}_{b,d}(k) = -\frac{i}{\sqrt{2\pi}} \left(1 - e^{ikd}\right) e^{-|k|b}, \tag{35}$$

and the magnitude of the Fourier transform of $F_{b,d}(x)$ is

$$\left|\tilde{F}_{b,d}(k)\right| = \frac{1}{k}\sqrt{\frac{2}{\pi}} \left| sen\left(\frac{kd}{2}\right)\right| e^{-|k|b}. \tag{36}$$

The behavior is illustrated in Figure 3, where we define the dimensionless variable $z = kd$ and the function,

$$g(z) = \sqrt{\frac{\pi}{2}} \frac{\left|\tilde{F}_{b,d}(k)\right|}{d}. \tag{37}$$

Note that $\lim_{z\to+\infty} g(z) = \frac{1}{2}$ and that $g(z)$ drops exponentially as z increases. For the fixed value of $b = 0.01d$, numerical analysis reveals that approximately 90 % of the total area of the graph occurs for $0 \leq z \leq 18\pi$.

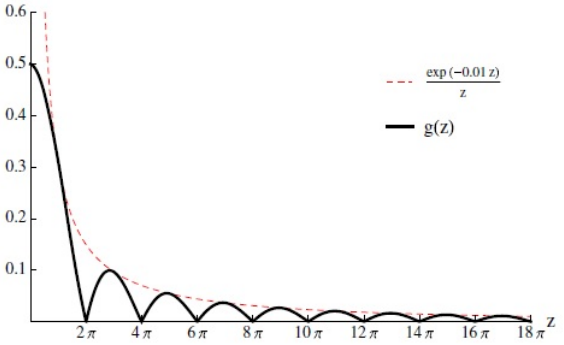

FIGURE 3. Fourier transform module of $\tilde{F}_{b,d}(x)$. Specifically, the function $g(z) = \sqrt{\frac{\pi}{2}}\frac{\left|\tilde{F}_{b,d}(k)\right|}{d}$ is plotted as a function of $z = kd$ for the case $b = 0.01$.

The approximations made require that (i) $\left|E^i\right| \ll \left|E^0\right|$, the dominance of the vacuum field over the background field,(ii) $\left|\nabla E^0/E^0\right| \ll \left|\nabla E^1/E^1\right|$, which is equivalent to $\lambda_p < \lambda_b$, (iii) a range of frequencies in which the material can be considered free from scattering, and (iv) a material that is approximately isotropic, at least for the frequencies that make the primary contribution to the background field. The decay rate of the Fourier transform $\tilde{F}_{b,d}(k)$ allows us to test approximations (ii) and

(iii). The exponentially decreasing behavior of the Fourier transform of this function, represented in Figure 3, suppresses the high energy modes of the background field in the material medium. For the case $b = 0.01d$, at least 90 % of the effect will occur in the range $0 \leq z \leq 18\pi$, which means that only wavelengths such as $\lambda_d \geq d/9$ will contribute significantly. For a plate with $d = 10\mu m$, the dominant wavelengths of the background field are those with $\lambda_b = 1.1\mu m$. Shorter wavelength modes are naturally suppressed by time averaging. Furthermore, the largest contribution occurs when it arises from $z \leqslant 2\pi$, which for $b = 0.01d$ in Figure 2, corresponds to a wavelength of $\lambda_b \approx 10\mu m$. Thus, if the material is relatively free from scattering when $\lambda_b \gtrsim 1.1\mu m$, then our assumption that n_b is frequency independent is justified,we can choose $\lambda_p \lesssim 1\mu m$ to satisfy the $\left|\nabla E^0/E^0\right| \ll \left|\nabla E^1/E^1\right|$.

Numerical Estimates for Cadmium Selenide (CdSe)

Cadmium selenide (Space Group: $P63mc$ (186), $a = 4.30$Å, $c = 7.01$Å and a hexagonal structure) is mainly employed for nuclear radiation detectors operating at room temperature, non-linear optical devices and as a substrate for epitaxial growth [17]. The material has a refractive index of $n_b = 2.43$, second-order susceptibility $\chi^{(2)}_{zzz} = \chi^{(2)} = 1.1 \times 10^{-10} mV^{-1}$ and a wavelength $n_p = 2.54$.

Among the semiconductor compounds II-VI, CdSe is an important material for the development of various modern solid-state device technologies, such as solar cells, high-efficiency thin-film transistors, light-emitting diodes, and etc.

CdSe has an energy gap of $1.80eV$ eV in the hexagonal (wurtzite) phase and $1.71eV$ and cubic zinc-blende phase, although it is metastable under normal conditions [18].

Generally, there are several methods of synthesis of CdSe (including Physical Plasma Spray Vapor Deposition (PS-PVD), sputtering, spray pyrolysis, electrodeposition, etc.)[19]. The synthesis method, by physical vapor deposition by plasma spray in its variants, is often used because it offers many possibilities for modification. Below, as illustrated in Figure 4, we have the hexagonal structure of the CdSe compound.

The thickness of the CdSe film for experimental analysis in nonlinear optics, has a range of $d = 0.10 - 1.80\mu m$), being measured using

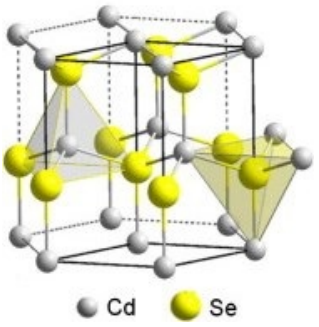

FIGURE 4. CdSe hexagonal structure.
Source: [20]

an interferometric method (Fizeau fringe methods for fringes of equal thickness). Now, setting the wavelength of the background field to $\lambda_p = 1.06\mu m$, for which $n_p = 2.54$, and setting the parameter $b = 0.01d$, we get from eq.(29) a fractional variation of the flight time [21],

$$\delta \cong 1.28 \times 10^{-8} \left(\frac{10\mu m}{d}\right)^2 \tag{38}$$

The optical dispersion in the refractive index in CdSe was normal and well described by a single oscillator model, in the absorption spectrum due to the effects of thermal fluctuations related in terms of indirect transitions [20]. Compared with the model where an idealized Lorentzian distribution is used, this result shows that in the situation described by $F_{b,d}(x)$, with $b = 0.01d$, the predicted effect is about 100 times more strong. This increase arises because the contribution to δ due to linear electric field fluctuations is proportional to $1/(bd)$, as can be seen from the first term on the right hand side of eq. (30). Contributions from the rest (mixed plus thermal) involve dispersions in the thermal distributions, which consist of the total contribution, that is, the total contributions of the system (remainder plus vacuum) to second-order terms accompanied by a mixed vacuum term. Note, it can take on larger values; since these mixed contributions are suppressed and the vacuum term dominates over the thermal term and successively over the mixed one, thus recovering the case of zero temperature. The graphic result of Figure 5 was generated using simulate calculation with the values for n_p, n_b, $\chi^{(2)}$, b and d given above. The value of $\gamma = \langle \Delta t_d^2 \rangle_\beta - \langle \Delta t_d^2 \rangle_0 / \langle \Delta t_d^2 \rangle_0$ for the vacuum contributions are dominant

in for negative values obtained from eq.(39), where represent on the vertical axis with the letter for γ, where we have to

$$\gamma = \frac{\langle \Delta t_d^2 \rangle_\beta - \langle \Delta t_d^2 \rangle_0}{\langle \Delta t_d^2 \rangle_0}, \tag{39}$$

$$\begin{aligned} I_x^T = \frac{n_b}{3\pi^2 {n_p}^2} Re \Bigg[2\frac{\Psi^{(1)}}{\beta^2}\left(\frac{\beta + 2n_p b}{\beta}\right) + \\ - \frac{\Psi^{(1)}}{\beta^2}\left(\frac{\beta - n_p(d+2ib)i}{\beta}\right) + \\ - \frac{\Psi^{(1)}}{\beta^2}\left(\frac{\beta + n_p(d-2ib)i}{\beta}\right)\Bigg], \end{aligned} \tag{40}$$

which resulted in the graphic obtaining of the Figure for the hexagonal structure of CdSe.

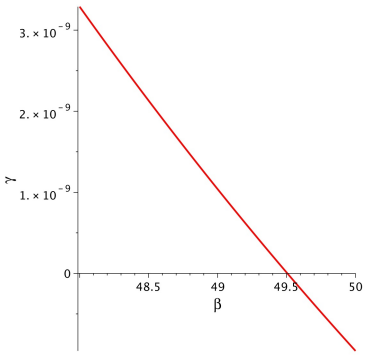

FIGURE 5. Flight time fluctuations γ versus temperature β for contribution of second order terms of the total−vacuum system for cadmium selenide (CdSe).

The result of the graph in Figure 4, was obtained using maplesoft. A simulation of this finite temperature calculation is:

$$\beta > 49.5\mu m = 49.5 \cdot 10^{-6} m, \tag{41}$$

$$\frac{1}{T} > 49.5\mu m \rightarrow T < 2 \cdot 10^4 m^{-1}, \tag{42}$$

$$\begin{aligned} 1K &- 4.37 \cdot 10^2 m^{-1} \\ T &- 2 \cdot 10^4 m^{-1} \end{aligned} \tag{43}$$

$$T < \frac{2 \cdot 10^4 m^{-1}}{4.37 \cdot 10^2 m^{-1}} K \rightarrow T \lessapprox 46K. \tag{44}$$

In part, the thermal contribution would be reduced for sufficiently long flight times at room temperature. We show that, at the low temperature limit, the contribution of thermal fluctuations to time-of-flight fluctuations is in low-temperature. When compared in the high-temperature regime the value of the numerical temperature estimate obtained from $T \lessapprox 46K$ for the inorganic compound of CdSe, are dominant byy vacuum fluctuations. While in the high-temperature limit, the contribution of thermal fluctuations to fluctuations in time of flight increases linearly with temperature, which dominates over vacuum fluctuations. Numerical estimates show that for cadmium selenide (CdSe) at room temperature, it shows that contributions from thermal fluctuations are still small compared to vacuum fluctuations in realistic situations. The vacuum contribution is only second-order terms in the convergent sum, the contribution is suppressed earlier, and the dominant vacuum becomes prominent. These vacuum effects will dominate thermal fluctuations for temperatures $T \lessapprox 46K$. These results can, in principle, be tested in the laboratory.

Conclusions

The main conclusions of this article are as follows:

- Vacuum electric field fluctuations undergo variations in the time of flight of the light pulse through a material with an effective refractive index.
- Therefore, thermal and mixed fluctuations are unavoidable in a real experiment, as they strongly contribute to the time-of-flight fluctuations in a material that has first- and second-order susceptibilities in a vacuum.
- Materials with second order susceptibility, $\chi^{(2)}$, provide the best results for the effects of thermal and mixed fluctuations.
- In a non-linear medium, effective refractive index for the light pulse is driven by vacuum fluctuations when the medium is subjected to a fluctuating background field, which leads to fluctuating time of flight.
- Furthermore, quantum fluctuations in the speed of light in a nonlinear material are a topic of interest in their own right.

- The numerical temperature estimate value obtained from $T \lessapprox 46K$, for the inorganic compound of CdSe at room temperature, shows that the contributions of the thermal fluctuations are still small compared to the vacuum fluctuations in realistic situations.

Acknowledgments

The authors would like to thank the Academic Unit of Physics and the Graduate Program in Physics of the Federal University of Campina Grande.

References

[1] E. Nelson, *Quantum fluctuations* (Princeton University Press, 1985).

[2] F. Benati, F. Carollo, R. Floreanini, and H. Narnhofer, J. Phys. A: Math. Theor. **50**, 423001 (2017).

[3] F. Intravaia, C. Henkel, and M. Antezza, Casimir Physics **834**, 345 (2011).

[4] D. A. Dalvit, P. A. M. Neto, and F. D. Mazzitelli, Casimir Physics **834**, 419 (2011).

[5] P. W. Milonni, *The quantum vacuum: an introduction to quantum electrodynamics* (Academic press, 2013).

[6] J. Hu and H. Yu, Phys. Rev. D **100**, 026009 (2019).

[7] J. Hu and H. Yu, Phys. Lett. B **777**, 346 (2018).

[8] A. Liu, S. L. Chuang, and C. Z. Ning, Appl. Phys. Lett. **76**, 333 (2000).

[9] M. Kauranen, J. J. Maki, T. Verbiest, S. Van Elshocht, and A. Persoons, Phys. Rev. B **55**, R1985 (1997).

[10] C. B. Schroeder, C. Benedetti, E. Esarey, and W. Leemans, Phys. Rev. Lett. **106**, 135002 (2011).

[11] C. Riek, D. V. Seletskiy, A. S. Moskalenko, J. F. Schmidt, P. Krauspe, and S. Eckart, Science **350**, 420 (2015).

[12] T. S. Evans and D. A. Steer, Nucl Phys B **474**, 481 (1996).

[13] D. Goderis, A. Verbeure, and P. Vets, J. Stat. Phys. **56**, 721 (1989).

[14] L. Robledo, Phys. Rev. C **50**, 2874 (1994).

[15] M. Cassier, P. Joly, and M. Kachanovska, Comput. Math. with Appl. **74**, 2792 (2017).

[16] L. Ford, G. De Lorenci, V.and Menezes, and N. Svaiter, Ann. Phys. **329**, 80 (2013).

[17] C. Bessa, V. De Lorenci, L. Ford, and N. Svaiter, Ann. Phys. **361**, 293 (2015).

[18] S. Suresh and C. Arunseshan, Appl. Nanosci. **4**, 179 (2014).

[19] B. Jensen and A. Torabi, J Opt Soc Am B. **3**, 857 (1986).

[20] G. Han, L. Wang, and et al., J. Alloys Compd **610**, 62 (2014).

[21] L. Ford and N. Svaiter, Phys. Rev. D **54**, 2640 (1996).